Protein Analysis in Cell Lines Retrovirally Infected with Oncogenic E7 Protein Variants from High-Risk HPV

Naomi I. Armstead

Submitted in partial fulfillment of the requirements for graduation as an Honors Scholar at

Point Loma Nazarene University, San Diego, California, May 6, 2023

Approved by _____

Dr. Heidi R.K. Woelbern

_____

Dr. Michael Dorrell

_____

Dr. Ariane Jansma

Date: _____

Abstract

The Human Papillomavirus (HPV) contains more than 200 serotypes of which 15 are classified as high-risk HPV. These high-risk serotypes are associated with cancers of the cervix, anus and penis. HPV encodes a viral oncoprotein, E7, that degrades retinoblastoma (pRb), a known tumor suppressor. Previous experiments have demonstrated significant decreases in pRb expression in cells infected with high-risk HPV16. This project aimed to investigate the molecular mechanisms by which E7 causes tumorigenesis. Specifically, this research studied the hydrophobicity and phosphorylation of high-risk HPV16 E7. Mutations were made to HPV16 E7 to test its functionality - one aimed to increase hydrophobicity and the other to increase phosphorylation. BJ cells, a human epithelial cell line, were retrovirally infected with the HPV16 E7 variants. It was observed that pRb degradation was diminished with a concomitant increase in hydrophobicity.

Background

Human Papillomavirus (HPV) is a double-stranded DNA virus that can be spread through skin-to-skin contact. It is the most common sexually transmitted infection in the United States with 14 million new cases per year [1]. Additionally, around 80% of sexually active people will contract HPV in their lifetime. The majority of infected men and women do not present clinically significant symptoms [2]. Viral infections, including HPV, cause approximately 15-20% of all human cancers. These oncogenic viruses increase the likelihood of cancer development [3]. Viruses are intracellular parasites that require a host cell to reproduce. Within the host cell, the viral genome can be transcribed allowing oncogenic proteins to be produced. These proteins hijack the host cell's own machinery to optimize viral production by increasing cell proliferation.

As of 2018, there are more than 200 known strains of HPV with 15 classified as "high-risk" while others are considered "low-risk" [4]. Low-risk HPV strains cause benign skin lesions while high-risk strains cause malignant tumors [4]. Of HPV infections, 50% contract a high-risk HPV strain [5]. Typically, the majority of HPV infections resolve by themselves within two years [2]. However, high-risk strains tend to have prolonged infections and increase the chance of cancer development. High-risk HPV causes almost all cervical cancers resulting in approximately 240,000 deaths worldwide annually [3]. Additionally, 70% of these cases involve the high-risk HPV16 and HPV18 serotypes [4].

HPV-based cervical cancer is primarily associated with the oncogenic protein E7 of high-risk HPV16 [6]. E7 has a promiscuous binding activity that is commonly found in viral proteins. It is an intrinsically disordered protein that is composed of three conserved regions. The intrinsically disordered regions (IDR) E7 from both low-risk and high-risk serotypes have a distinct binding motif to an LXCXE segment of tumor suppressor retinoblastoma (pRb) [6]. E7 is, therefore, able to debilitate functioning pRb (**Figure 1**). As pRb functionality is impaired, the transcription factor E2F is released and initiates cell proliferation [6]. This release can result in cell proliferation which is associated with tumor progression. The oncoprotein E7, therefore, has a significant role in causing cancers linked to HPV.

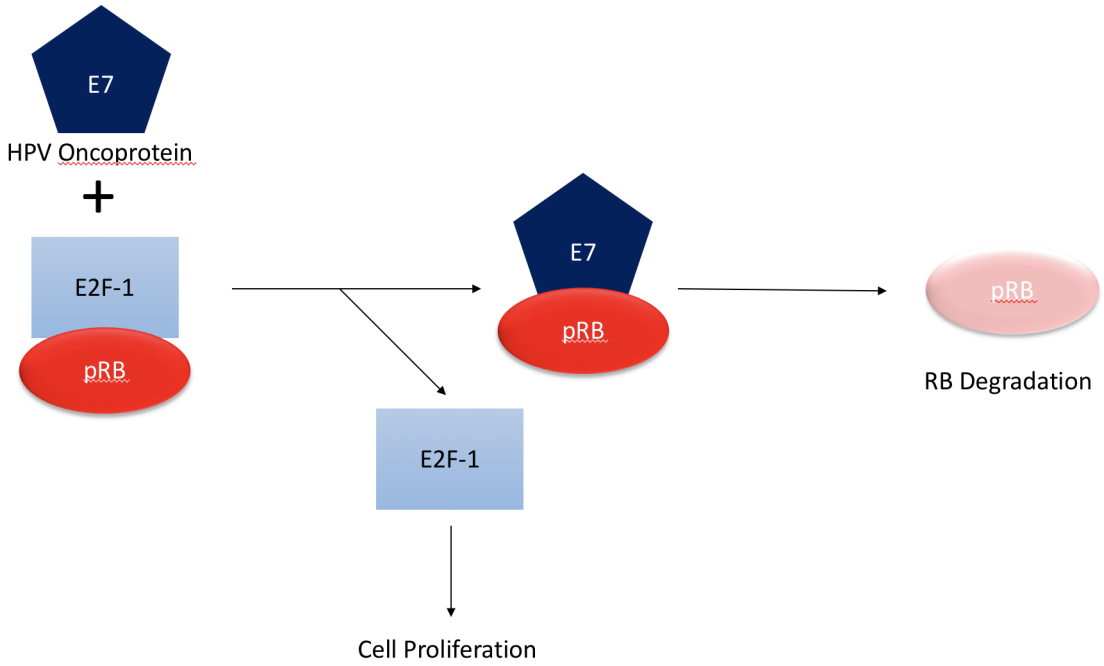

Figure 1. Cell proliferation due to E7 HPV protein: The binding of E7 and pRb, degrading pRb and displacing E2F. E2F is then released to enter the nucleus and promote cell division which decreases inhibition of the cell cycle.

It has been established that low-risk HPV6b E7 has a decreased affinity for pRb compared to HPV16 and does not as effectively function in tumorigenesis [7]. The mechanism by which high-risk E7 dysregulates the cell cycle has yet to be fully understood. Current research is focused on investigating the differences between low-risk and high-risk E7 to better understand their different phenotypic outcomes. Some research indicates the significance of serine residues that are downstream of the LXCXE binding motif (**Figure 2**) and their role in E7's phosphorylation ability [7]. This motif is found in the second conserved region of E7's IDR [6]. IDRs of proteins are readily exposed to a polar aqueous environment. So, sequences with higher polarity would be more stable within the cell. Therefore, phosphorylation through serine, threonine or tyrosine residues could stabilize high-risk E7 and increase its efficiency in binding to pRb [8]. For this reason, it is important to study how phosphorylation efficiency and hydrophobicity levels in different E7 variants correlate with pRb degradation in relation to cancer risk levels.

Previously, this lab has established and researched stable HPV cell lines transfected with an HPV plasmid (pLXSN), HPV6b (low-risk) and HPV16 (high-risk) variants. pRb degradation in retrovirally infected HT1080 and BJ cell lines has been visualized in past experiments. This study used the HPV16 E7 sequence (highlighted in orange) to introduce mutations that targeted hydrophobicity and phosphorylation (**Figure 2**). All mutations are depicted within the pink box in **Figure 2**. The amino acids within the pink box are the phosphorylation recognition sequences. This recognition sequence was targeted for mutations as it was aimed to change the ability of E7 to degrade pRb due to phosphorylation. One mutation was made at position 29 to change an asparagine (N) to a valine (V). A second valine

was inserted at position 36 (+35V36) to make the HPV16 E7 sequence more similar to HPV6b which has more hydrophobic residues. This variant is called the Double-Mutant (DM) and is considered “low-risk acting” as it was expected to decrease the degradation of pRb. These two valine mutations are seen in the DM sequence above the orange highlighted HPV16 sequence. Then oppositely, a second variant was produced to make an ultra-high-risk E7. To achieve this, N29 was mutated to a serine (S) that has phosphorylation capabilities. This variant is called Ultra (N29S) as this variant is naturally occurring but is even higher risk than HPV16. The mutation can be seen in the sequence below HPV16 (**Figure 2**).

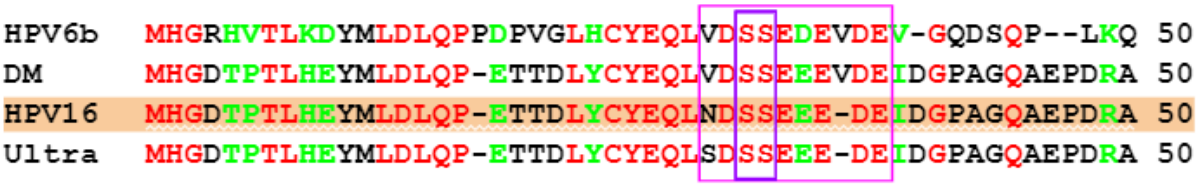

Figure 2. E7 variant sequences: Amino acid sequences of residues 1-50 are shown above. HPV16 is highlighted in orange as that is the sequence used to establish the DM and Ultra variants. The pink box sections off where the specific mutations were made. The DM and HPV6b sequences are aligned to display their similarities. The red-colored amino acids are identical and the green ones have similar properties.

The BJ cell line was retrovirally infected with the DM and Ultra HPV variants that were established in this study. The BJ normal (no transduction), pLXSN, low-risk, high-risk, DM and Ultra cell lines were characterized and the degradation of pRb was visualized using western blot analysis. Additionally, E7 variants were analyzed through qPCR to confirm that the correct genes were present in each BJ HPV variant.

Materials and Methods

HPV Constructs

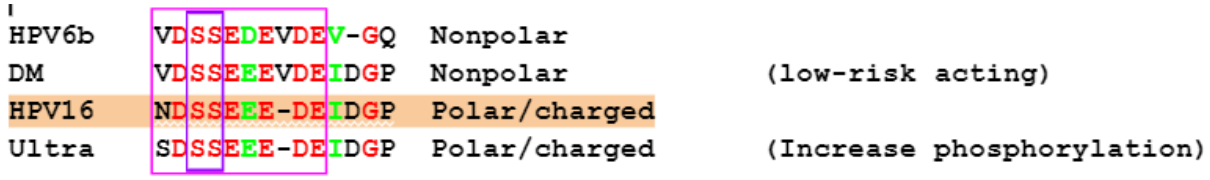

Figure 3. Localized HPV E7 variant sequences:

The high-risk HPV16 E7 and low-risk HPV6b E7 plasmids used in retroviral infection of BJ cells were obtained from the plasmid repository Addgene. The HPV16 E7 plasmid can be found at this link: https://www.addgene.org/52396/. The HPV6b E7 can be found at this link: https://www.addgene.org/52398/.

The additional constructs were made using the high-risk HPV16 E7 plasmid in conjunction with site-directed mutagenesis (Agilent QuickChange II kit). The first construct obtained was the ultra-competent N29S construct, in which an asparagine (N) at position 29

was changed to a serine (S) by mutating its codon from AAT to AGT (see primers utilized in **Figure 2**). The double mutant (DM) construct required a two-step process. The first mutation also targeted N29 but changed it to a valine (N29V) by mutating the codon to GTT. The second mutation was an insertion of a valine at position 36 (+35V36). Constructs were transformed into competent cells, plasmids were purified and confirmed by sequencing.

Viral Constructs:

The Moloney murine leukemia virus (MMLV) retroviral particles used in this research were synthesized by VectorBuilder. Packaging, storage information, and protocols can be found here: https://en.vectorbuilder.com/products-services/service/mmlv-retrovirus-packaging.html.

Cell Culture:

BJ cells were maintained in media consisting of EMEM, 10% FBS, 1X Anti-Anti and 300ug/mL of G418 in a 5% CO_2 incubator at 37°C. Cells were split every 3-5 days depending on growth.

Viral Transduction/GFP imaging:

Before viral transduction (Day 0), four T25 (25cm^2) flasks were plated with BJ cells at 3.5x10^5 cells/flask and grown to 30-50% confluency. For transduction (Day 1), media (EMEM+10%, FBS, without ANTI-ANTI) was supplemented with 5ug/ul of polybrene. Previous studies indicated that polybrene had no obvious toxicity for 72 hours up to 10ug/ul. The appropriate amount of virus was added to the polybrene-supplemented media for a final volume of 2.5mL (**Table 1**). The old medium was replaced from the target cells with the virus-containing media and incubated at 37°C in a humidified 5% CO_2 incubator for 6 hours. 1mL of media (EMEM+10%, FBS, without ANTI-ANTI) was added to each flask after 6 hours and incubated overnight. On day 2, the virus-containing medium was removed and the BJ cells were split from a T25 flask to a T75 flask to be grown in a complete culture medium (EMEM+10%, FBS, and ANTI-ANTI). Day 3, selection began by using G418 media (EMEM+10%, FBS, ANTI-ANTI, 300ug/mL G418) and replacing media every 2-3 days. For the EGFP flask, 2ug/mL of puromycin was used for selection instead of G418. By day 11, the selection was complete which was indicated as no BJ (no transduction control flask) remained. The data and protocol for HPV E7 infection including the time course, dosing, and additional protocols can be found here: TRANSDUCTION OF BJs w/ VIRAL HPV16 E7.

Table 1: Amount of virus used to establish stable cell lines.

T25 FLASK	CELLS	#cells seeded	VIRUS	TU/ml	Amount Virus in ul (MOI-2.5)	Media w/polybrene (5ug/ul)
1	BJ	3.5x10^5 cells	None			2500 ul
2	BJ	3.5x10^5 cells	pLXSN_HP V16 E7_DM	1.57x10^7	55.7 ul	2444 ul
3	BJ	3.5x10^5 cells	HPV16-E7_ N29S	6.16x10^7 TU/ml	14 ul	2486 ul

4	BJ	$3.5x10^5$ cells	MMLV_EGFP	$7.22x10^7$ TU/ml	12.1 ul	2488 ul

The stable GFP line was split into a second flask. One flask continued to be selected with puromycin and the second had no selection. The GFP BJ cells were plated onto two chamber slides for GFP visualization to confirm that transduction was successful at different concentrations per well (**Tables 2,3**).

Table 2: Chamber Slide BJ without puromycin selection

Well	Number of Cells	ul of stock (6.4x105cells/mL)	mL of media (up to 0.5mL)
1	$2.5x10^4$ cells/well	39	461
2	$5x10^4$ cells/well	78	422
3	$7.5x10^4$ cells/well	117	383
4	$1x10^5$ cells/well	156.25	344

Table 3: Chamber Slide BJ with puromycin selection

Well	Number of Cells	ul of stock ($1.8x10^5$cells/mL)	mL of media (up to 0.5mL)
1	$2.5x10^4$ cells/well	139	361
2	$5x10^4$ cells/well	278	222
3	$7.5x10^4$ cells/well	417	83
4	$1x10^5$ cells/well	556	0

The slides were incubated at 37°C in a CO_2 chamber for 24 hours. After incubation, the cells were washed with PBS and then fixed with 4% PFA. A second wash was done with PBS before nuclear staining by PBS+DAPI for 10 minutes. Once staining was complete the wells were removed to mount the cells with anti-fade and a glass cover. The slides were then visualized through fluorescent microscopy. The protocol for GFP visualization including the time course, dosing, and additional protocols can be found here: GFP 2022.

Protein Analysis by Western Blots:

The expression of pRb in the six stable cell lines was analyzed through western blotting. Cell lysates were obtained by using RIPA buffer that included protease inhibitors. The lysates were centrifuged at 14,000xg to isolate proteins. Protein concentrations were determined through a standard BCA protocol: Protocols for Protein Analysis.

Four western blots were performed for each lysate group obtained from six stable BJ cell lines: BJ (no transduction), pLXSN (plasmid control), low-risk (HPV6b), high-risk (HPV16), N29S (ultra), and the Double Mutant (DM). For the ladder, 3uL of the iBright Prestained Protein Ladder (Thermo Scientific) was used. As a positive control, 10ng of Recombinant Rb (Sigma-Aldrich, catalog number: SRP2081- 5µg) was added with 2.5µL of LDS sample buffer (Invitrogen), 1µL of Bolt Reducing Agent (Invitrogen), and 5.5 ul of Milli-Q water. Lysate samples were prepared by using 8.75µL LDS, and 2.5µL Bolt Reducing Agent with the appropriate µg of protein according to the lysate group. Additionally, Milli-Q water was added to bring each sample up to 22.75µL total. All lysate samples, excluding the ladder, were incubated in a water bath at 70°C for 10 minutes. All samples were loaded into a Bolt 4-12% Bis-Tris Plus gel (Invitrogen) that was run at 200V and 40mA for approximately one hour. The protein bands were transferred to an activated tris-glycine PVDF membrane (with methanol for 30 seconds) through a blotting sandwich. The blot sandwich was constructed in this order: cathode core, sponge pad, filter paper, Bolt gel, PVDF membrane, filter paper, two sponge pads, and anode core. The sponges and filter paper were soaked in Transfer Buffer prior to assembly. The transfer was run at 20V and 160mA for 1 hour. After the transfer was complete, the membrane was washed with Milli-Q water and then blocked in milk buffer for at least 3 hours. Following the initial block, the membrane was transferred into a primary milk buffer solution of 1:500 Rb antibody (Catalog number: ab181616) and 1:2500 GAPDH (ThermoFisher, catalog number: MA515738). GAPDH was used as a normalization factor for a control. The membrane was left in the primary antibody overnight on a tilting platform at 4°C. The following day, the membrane was washed from the primary antibody 6 times using TBST. The membrane was then transferred into a secondary antibody solution of 1:10,000 Rb Goat anti-Rabbit IgG (HRP Catalog Number: 31460) and 1:2000 GAPDH Goat anti-Mouse IgG HRP to bind to their respective primary antibody. It was washed in the secondary antibody for 1 hour. After this, the membrane was washed 5 times in TBST and then was activated in a peroxide Luminol/ Enhancer working solution. The Rb and GAPDH protein bands were visualized on a chemiluminescence setting on an imaging machine.

To measure the percent expression of pRb, the visualized bands were analyzed through ImageJ.

RNA Isolation and qPCR:

RNA was isolated utilizing the Zymogen Micro Plus kit. All cell lines were grown to around 100% confluency, except pLXSN which was around 80%, for approximately 6×10^6 cells total per line. RNA concentrations were determined using nanodrop (**Table 5**). Reverse transcription was performed on all isolations using the Invitrogen SuperScript IV First-Strand Synthesis System procedure and kit. Each reaction ran with 1.5 µg of RNA with the HPV6b concentration being the limiting factor. 1 ul of E. coli RNase H was used to remove RNA from the controls and each sample. To confirm that the reverse transcription was successful, a cDNA amplification and gel electrophoresis was run for the control and BJ cDNA (**Figure 10**). In order to quantify and analyze E7 variant gene expression a qPCR was run for cDNAs from the normal, pLXSN, low-risk, high-risk, DM, and N29S BJ variants. The qPCR amplification reactions contained SYBR Green PCR master mix (Bio-Rad) and primers. GAPDH was used as a reference gene. The six variants were run with high-risk E7 and low-risk E7 primers. The gene

expression was quantified through the comparison of threshold cycle values. Then, data were analyzed by double normalization. First, the data were normalized to the reference gene, GAPDH, and then relative expression levels were calculated.

Results

Mutated DNA Sequences:

Gel electrophoresis was used to determine the presence of the desired mutation in the DNA mutated to N29S (1), N29V (2) and +35V36 (3) (**Figure 4**). Bands from the three mutated DNA samples were observed at 688, 1055, 1911, and 2585 bp. Samples from 1 and 2 had strong bands while samples from 3 showed faint bands. 1A-E, 2A-C, E and 3B-E all had bands at the proper position thus likely expressing the proper mutations. 2D and 3A did not show these bands and therefore did not uptake the plasmid. DNA sequences 1A, 2A and 3B were selected to be analyzed and confirm that the correct mutation was present through sequencing.

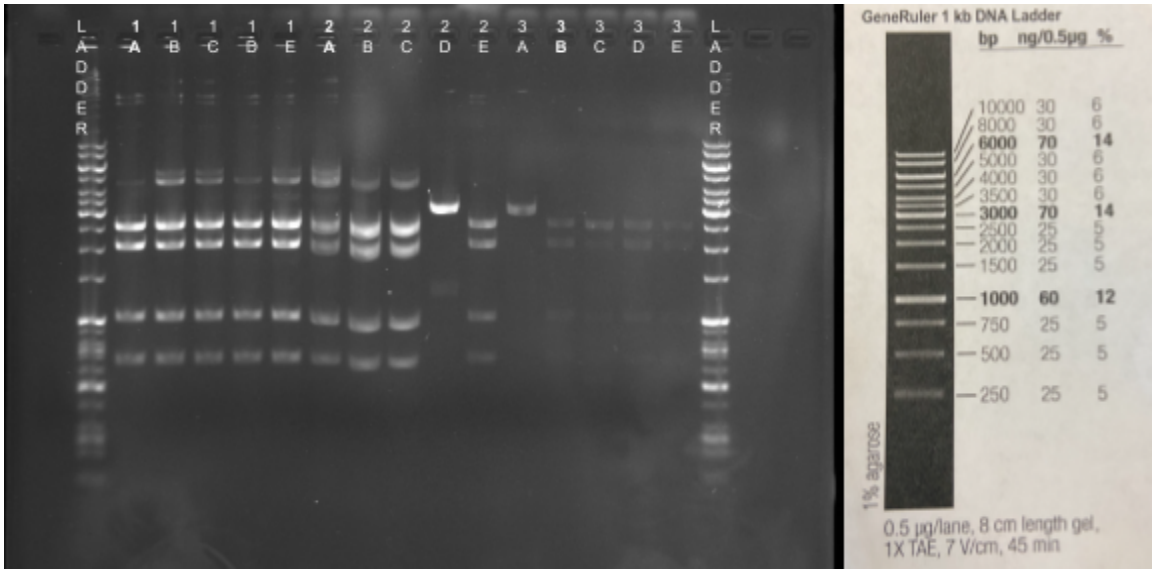

Figure 4. Gel electrophoresis of Mutated HPV16 E7 DNA: All three mutated DNA sequences were run on a 2% Agarose gel with 5 samples each (A-E). A 1kb DNA Ladder was used to track the position of the bands with markers to 688, 1055, 1911, and 2585 bp.

DNA from 2A (N29V) and 3B (+35V36) were used to produce the DM as the fourth mutated sequence (**Figure 5**). +35V36 was used as a template for site-directed mutageneis with N29V primer. Samples 4B-4E had a successful mutation for the DM as seen by the four bands at around 688, 1055, 1911, 2585 kb. These samples were further sequenced to confirm that they had the proper mutations in the proper position.

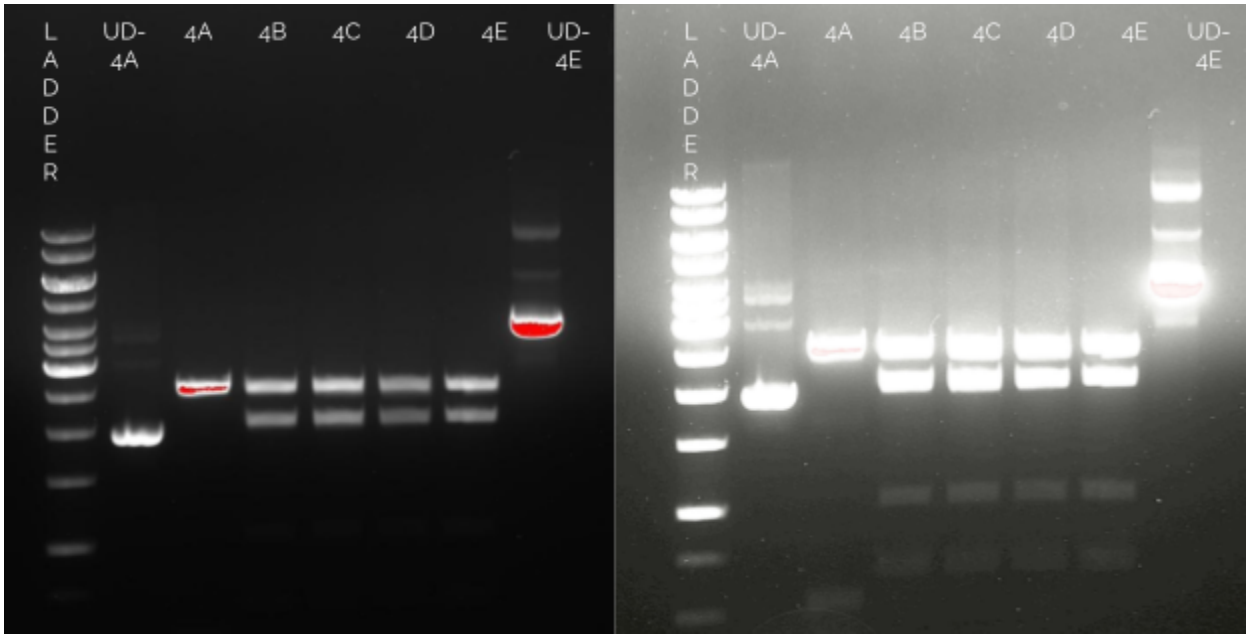

Figure 5. Gel electrophoresis of Double Mutant DNA:
Five samples (A-E) of the DM (4) sequence were run on a 2% Agarose gel along with undigested UD 4A and 4E as controls. A 1kb ladder was also used to determine the positioning of bands. 4B-4E has four bands that indicate the desired mutations.

Transduction with HPV Variants:

The success of transduction was tracked by comparing the growth of the three BJ strains through selection by G418. By day 11 of transduction there were no surviving control BJ cells (**Figure 6a**) but cells infected with the DM (**Figure 6b**) and N29S (**Figure 6c**) were healthy and growing. Since the control cells were completely dead, this indicated that the DM and N29S cells had successful transduction. This is because the plasmids were designed with resistance against G418, so any surviving cells have taken up the mutated DNA.

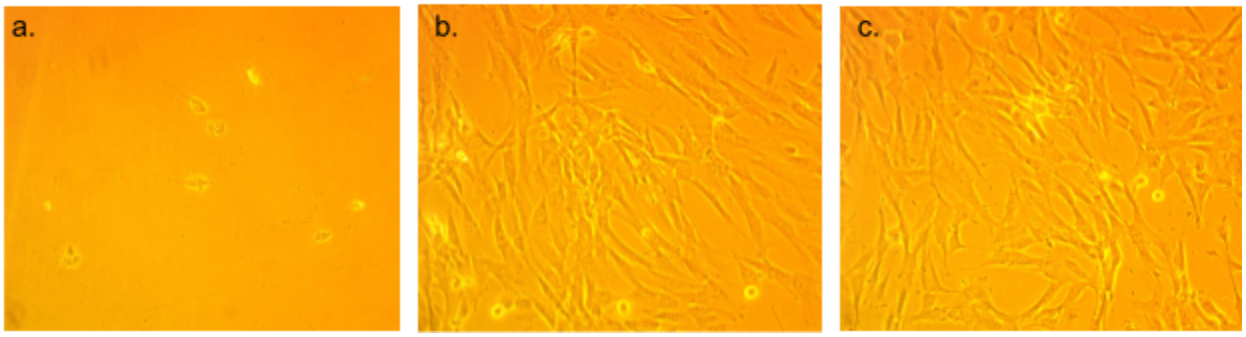

Figure 6. Images of BJ stables under G418 selection on Day 11:
a) Control BJ cells (no virus). b) BJ-HPV16 E7 Double Mutant. c) BJ-HPV16 E7 N29S

To further confirm transduction success, stable cells that were infected with GFP were visualized through immunohistochemistry. The fluorescent microscopy images in **Figure 7** are representative of images taken of BJ cells 9 days post-infection with 4 days of selection with

puromycin. Cells successfully infected with GFP will fluoresce green whereas all nuclei will fluoresce blue with DAPI. **Figure 7a** shows very little expression of GFP in the BJ stables when there was no puromycin selection. On the other hand, BJ stables selected with puromycin (**Figure 7b**) had high expression of GFP. This again confirmed that the transduction conditions of the new BJ stables were successful.

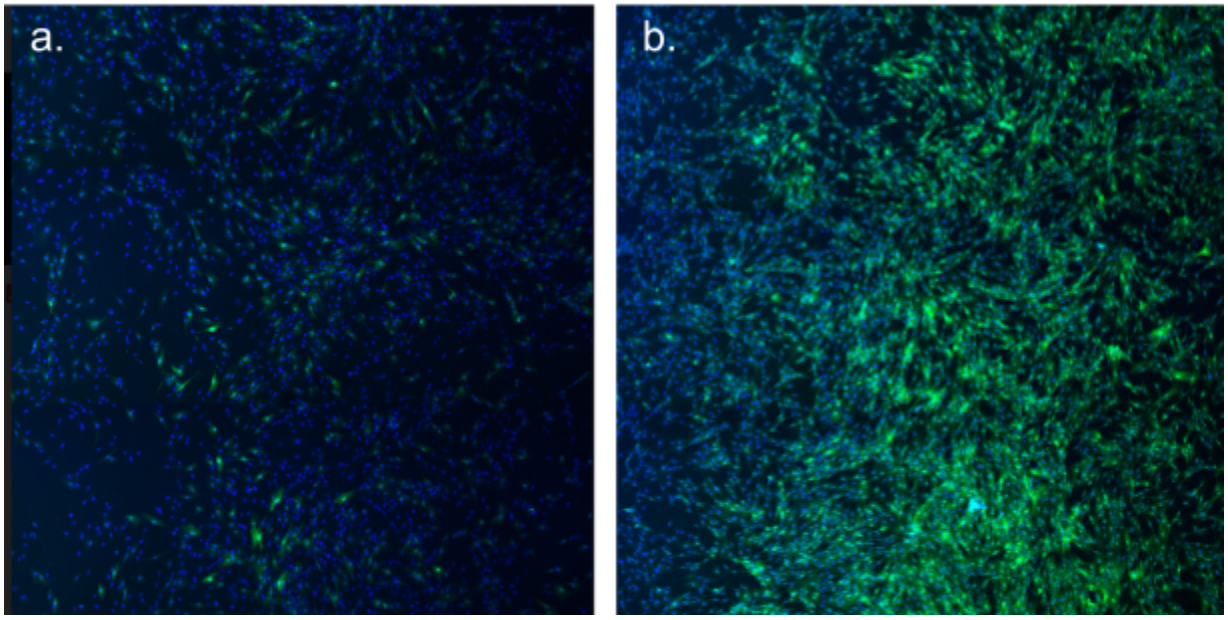

Figure 7. Visualization of Stable BJ Lines Infected With GFP: To confirm the successful transduction of established BJ cell lines, two groups of GFP-infected cells were stained for DAPI and GFP. Image a. displays BJ cells infected with GFP without puromycin selection. Image b. Displays BJ cells infected with GFP under puromycin selection.

Western Blot Analysis:

Once two new HPV-infected cell lines were established (HPV DM and HPV N29S), along with the Normal, pLXSN, HPV6b, and HPV16, western blotting was used to characterize protein expression in the cell lines. It has been shown that there is an increased degradation of pRb by the high-risk HPV16 E7 as compared to low-risk HPV6b E7. Additionally, specific conserved DNA sequences are believed to play a significant role in the function of high-risk HPV16 E7. Phosphorylation is suspected to be directly correlated with E7's ability to degrade pRb. So, the HPV16 E7 N29S mutation, which should increase phosphorylation, should in turn cause an increase in pRb degradation. Oppositely, hydrophobicity is believed to have an indirect correlation with the degradation of pRb. So, increasing hydrophobic amino acids should decrease the degradation of pRb and the high-risk E7 should function more similarly to low-risk E7. Within this line of thinking, HPV DM E7 would decrease in pRb degradation compared to HPV16 E7 as two more valines were added to the sequence.

In a western blot, the darkness/thickness of the bands correlates to the expression of that protein when normalized. It is known that high-risk HPV16 E7 increases pRb degradation more than low-risk HPV6 E7. So, it was expected that HPV6b should have a darker thicker band when compared to HPV16. The DM was also expected to have a thicker band than the HPV16 and be more similar to HPV6b. The N29S was expected to have the thinnest band out of each

variant as it has higher phosphorylation efficiency. The pLXSN lysate was run along with the other variants to ensure that the plasmid infection did not impact pRb levels. GAPDH was used as a normalization factor to ensure equal loading of cell lysates per well. On average, the four western blots displayed a trend that matches the expected results (**Figure 8**). The visual trend was quantified by using ImageJ to calculate the percent expression of pRb.

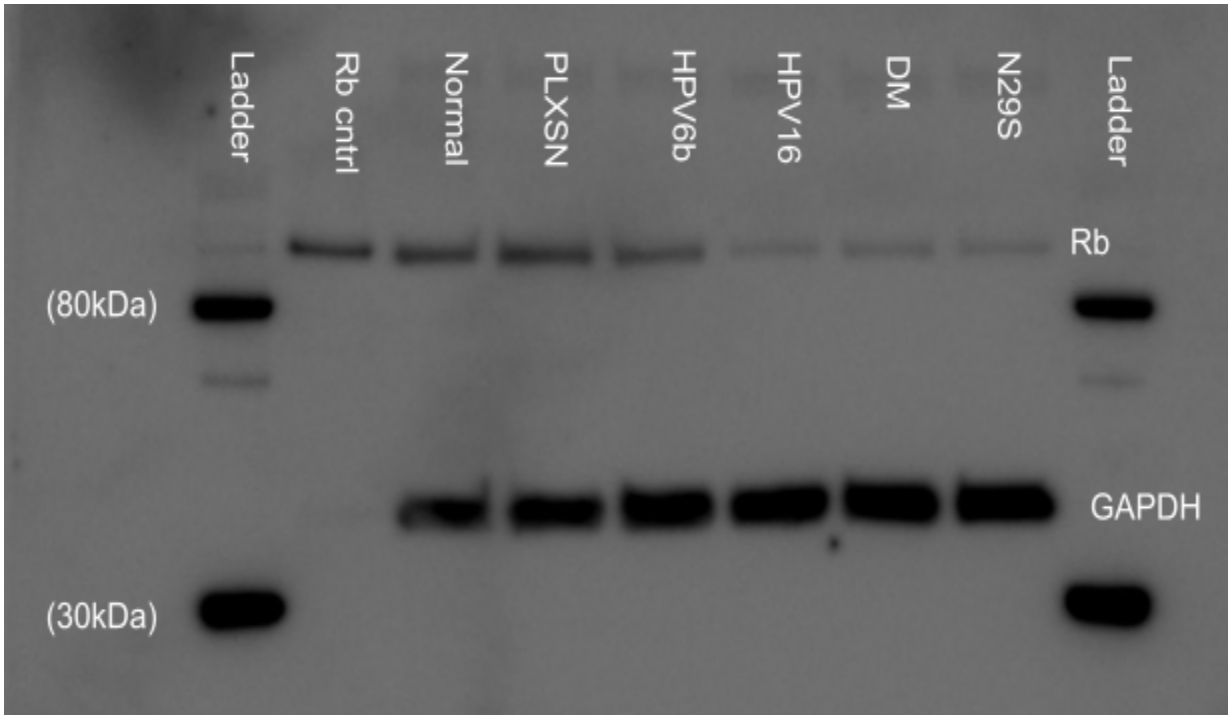

Figure 8. Western blot of pRb and GAPDH from six stable BJ cell lines: Protein was isolated from Normal, pLXSN, HPV6b, HPV16, DM, and N29S (ultra) infected BJ cultures. pRb recombinant protein was used as a positive control. Rb is the top row of bands at 110 kDa. GAPDH is the bottom row of bands and was used as a normalization factor at 37 kDa. A ladder with bands at and was used to standardize the size of the bands.

Averages of pRb expression were calculated and graphed onto the chart below (**Figure 9**). When normalized to PLXSN, it was seen across all four blots that HPV16 had lower pRb expression of 17.9% than HPV6b which was 47.8%. This further confirmed previous knowledge of E7 variants. On average there was a trend of the DM having higher expression (22.9%) than the HPV16, but lower than the HPV6b which was observed in **Figure 9**. Increased phosphorylation in the N29S variant was not seen to lead to an increase in pRb degradation. Yet, the other three blots all had higher pRb expression in the N29S variant compared to HPV16. It cannot yet be determined if this data is statistically significant. Yet, it does provide intriguing and encouraging information about the importance of the amino acid sequences in the targeted areas of HPV16 E7.

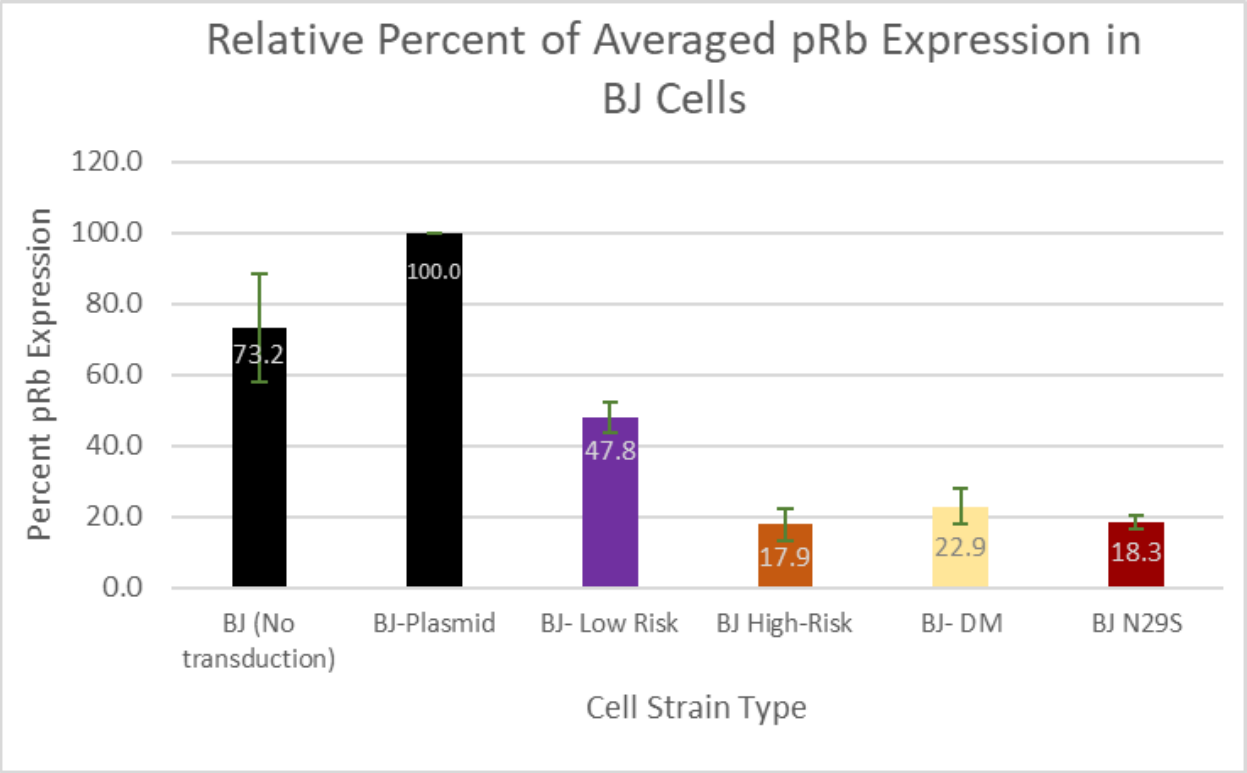

Figure 9. Average of pRb expression per variant from four western blots: Percent of pRb expression was calculated per blot from normalized pRb areas found through ImageJ. The graph presents averaged percentages based on the variant.

RNA Isolation and qPCR:

It has been difficult to analyze HPVE7 expression by protein analysis. In order to confirm that the E7 transcript was made, we conducted quantitative PCR analysis, utilizing E7 primers specific for the low-risk (HPV6b E7) and the high-risk (HPV16 E7) strains. The HPV16, DM, and N29S variants exhibited high expression of the HPV16 E7 primer and very low expression of HPV6b E7 as expected (**Figure 10**). This was expected as the DM and N29S variants were derived from the HPV16 sequence. So, there should be a minute cross-expression of HPV6b in these variants as seen in **Figure 10.** The HPV6b variant had high expression of its E7 and very low expression of HPV16. The housekeeping gene GAPDH was used as a reference gene. These data indicate significant expression of the appropriate E7 genes in each variant.

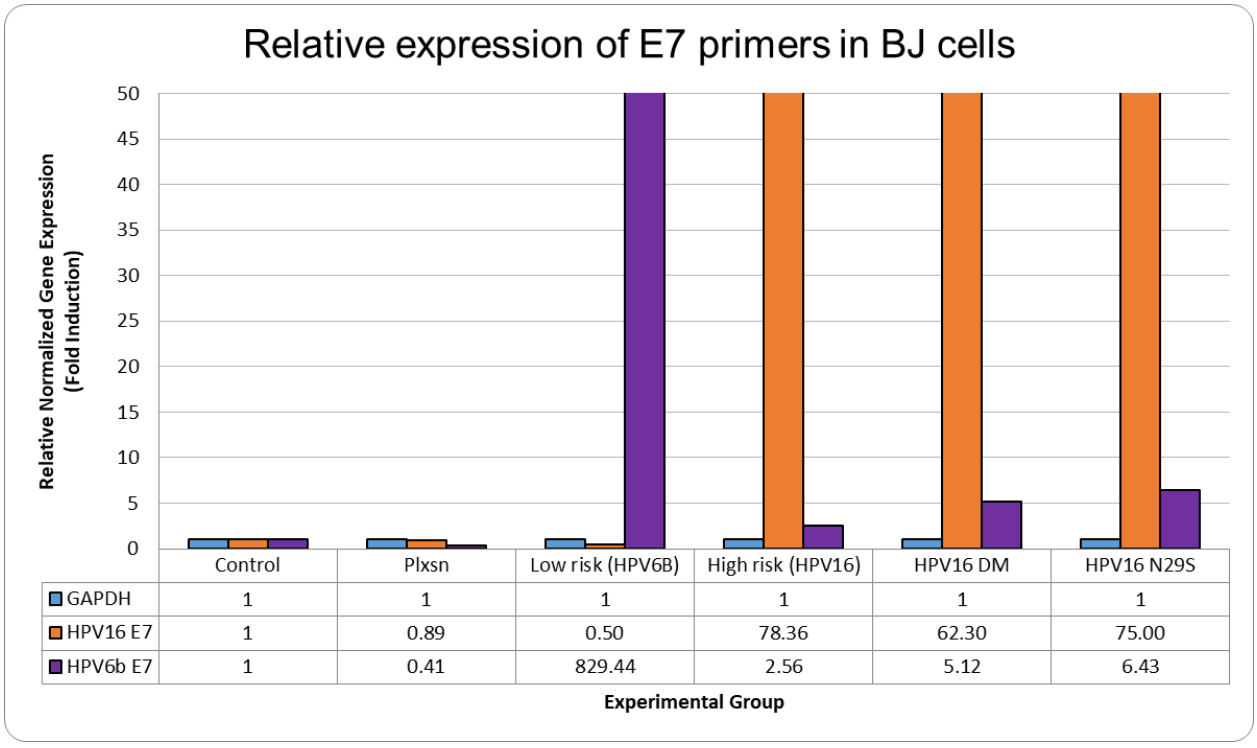

Figure 10. Expression of qPCR E7 primers in different HPV variants:
This figure contains graphical representations of the presence of HPV16 and HPV6b genes in the four variants. GAPDH was used as a normalization factor.

Discussion

Utilizing Site-Directed Mutagenesis, two new variants (DM and N29S) were successfully derived from the high-risk HPV16 DNA sequence (**Figures 2,3**). BJ cells were then successfully retrovirally infected with the DM and N29S variants (**Figure 6**). Standard cell culture practices were used to maintain these cell lines in addition to non-infected control BJ cells, as well as BJ cells infected with either pLXSN (vector control), low-risk and high-risk variants. The DM and N29S infected cells were frozen down for future analysis. The six cell lines were characterized using western blots to visualize the degradation of pRb by HPV protein E7. The western blots were also used to successfully quantify expression through Image J (**Figures 8,9**). The pRb degradation in the DM and N29S was successfully visualized and compared to the control pLXSN and any differences in degradation between the two mutants and HPV16 were observed. Additionally, the large difference in pRb degradation between HPV6b and HPV16 was further confirmed by the westerns obtained in this study. HPV16 and N29S degraded pRb at substantially higher levels than HPV6b in BJ cells. Although, the slight difference in pRb expression between the N29S and HPV16 variants could be due to the serine not adding significant phosphorylation capabilities to the E7 protein. Additionally, the serine may be in a position that, although phosphorylated, does not interact as strongly with pRb. Yet, this data does indicate the role of hydrophobicity between low-risk and high-risk E7. That is, an increase in hydrophobicity, as seen with the DM, decreases the ability of E7 to degrade pRb. The DM

also had substantially higher degradation compared to HPV6b but less compared to HPV16. Thus, two new HPV-infected cell lines were successfully established and characterized.

This data was further confirmed through RNA analysis by qPCR. The data confirmed that E7 RNA is transcribed in the established cell lines of retrovirally infected HPV6b, HPV16, DM, and N29S BJ cells (**Figure 10**). We presume the expression of E7 is responsible for the degradation of pRb observed by western blot analysis. So, the large decrease of pRb expressed in HPV16 is likely due to degradation by the high-risk E7 expressed in those cells. The less degradation seen in HPV6b can also be associated with low-risk E7.

To further study the role of hydrophobicity and phosphorylation within E7, a computational analysis will be performed through R Studio. Hydrophobicity and phosphorylation values can be assigned to amino acids that is used to calculate the overall levels of the two factors for a specific sequence. This is done by summing the assigned hydropathy values of each individual amino acid and then dividing it by the sequence length. This is called the grand average hydropathy known as a GRAVY score. The higher the GRAVY score the more hydrophobic the sequence is. It would be expected that HPV6b to have the highest GRAVY score, then the DM sequence, HPV16 and the lowest would be the N29S. Additionally, the same set of experiments would be performed on HT1080 cells that have already been retrovirally infected and established. This would hopefully confirm the current trends seen by this study.

Works Cited

[1] Manini I, Montomoli E. Epidemiology and prevention of Human Papillomavirus. Ann Ig. 2018 Jul-Aug;30(4 Supple 1):28-32. doi: 10.7416/ai.2018.2231. PMID: 30062377.

[2] Centers for Disease Control and Prevention. (2023, February 10). Human Papillomavirus HPV). Centers for Disease Control and Prevention. Retrieved March 14, 2023, from https://www.cdc.gov/hpv/parents/about-hpv.html

[3] Ntanasis-Stathopoulos, I., Kyriazoglou, A., Liontos, M., A Dimopoulos, M., & Gavriatopoulou, M. (2020). Current trends in the management and prevention of human papillomavirus (HPV) infection. J BUON, 25(3), 1281-1285.

[4] Chan, C. K., Aimagambetova, G., Ukybassova, T., Kongrtay, K., & Azizan, A. (2019). Human Papillomavirus Infection and Cervical Cancer: Epidemiology, Screening, and Vaccination-Review of Current Perspectives. Journal of oncology, 2019, 3257939. https://doi.org/10.1155/2019/3257939

[5] Okunade K. S. (2020). Human papillomavirus and cervical cancer. Journal of obstetrics and gynaecology : the journal of the Institute of Obstetrics and Gynaecology, 40(5), 602–608. https://doi.org/10.1080/01443615.2019.1634030

[6] Minnesota Department of Health . (2019, August). Quick facts: HPV-associated cancer. Quick Facts: HPV-Associated Cancer - MN Dept. of Health. Retrieved March 14, 2023, from https://www.health.state.mn.us/data/mcrs/data/qfhpv.html#:~:text=Around%2050%20percent%20of%20HPV,HPV%2C%20which%20can%20cause%20cancer.

[7] Lee, C., Kim, D. H., Lee, S. H., Su, J., & Han, K. H. (2016). Structural investigation on the intrinsically disordered N-terminal region of HPV16 E7 protein. BMB Rep, 49(8), 431-436. https://doi.org/10.5483/bmbrep.2016.49.8.021

[8] Heck, D. V., Yee, C. L., Howley, P. M., & Münger, K. (1992). Efficiency of binding the retinoblastoma protein correlates with the transforming capacity of the E7 oncoproteins of the human papillomaviruses. Proc Natl Acad Sci U S A, 89(10), 4442-4446. https://doi.org/10.1073/pnas.89.10.4442

[10]Jansma, A. L., Martinez-Yamout, M. A., Liao, R., Sun, P., Dyson, H. J., & Wright, P. E. (2014). The high-risk HPV16 E7 oncoprotein mediates interaction between the transcriptional coactivator CBP and the retinoblastoma protein pRb. J Mol Biol, 426(24), 4030-4048. https://doi.org/10.1016/j.jmb.2014.10.021